Available online at www.sciencedirect.com

SCIENCE DIRECT®

Materials Letters 59 (2005) 994–997

materials letters

www.elsevier.com/locate/matlet

Mesoporous titania: effect of thermal treatment on the texture and acidic properties

Luis René Pizzio*

Centro de Investigación y Desarrollo en Ciencias Aplicadas "Dr. J. J. Ronco" (CINDECA), Facultad de Ciencias Exactas, UNLP-CONICET, 47 No 257, 1900-La Plata, Argentina

Received 11 May 2004; accepted 12 November 2004
Available online 13 December 2004

Abstract

Mesoporous titania materials have been synthesized by using urea as low cost template via sol–gel reactions of titaniumisopropoxide, followed by removing the urea by extraction with water. They were characterized by FT-IR, XRD, DTA-TGA and BET. The S_{BET} of the solids increases with the increase of the urea content and decreases with the increase of the calcination temperature.

The XRD patterns of the samples exhibit only the characteristic peaks of the anatase phase. The crystallinity increased when the temperature went up.

The acidic characteristics of the samples were evaluated by TPD and DRIFTS of adsorbed pyridine. The total amount of pyridine adsorbed decreases in parallel with the increase of the calcination temperature. The samples displayed two types of Lewis acid sites, with which pyridine interacts via coordination bonding.

Keywords: Titania; Mesoporous; Sol–gel preparation; Catalysts; Thermal properties

1. Introduction

In 1990, Yanagisawa et al. [1] described the preparation of mesoporous silicas with uniform pore size, and the next year, researchers at Mobil Research and Development Corporation [2] reported the synthesis of aluminosilicates with unique pore size in the mesoporous range. Since then, mesoporous materials have attracted much attention in several fields related to catalysts preparation because of their high specific areas and pore size distributions. They have been synthesized via sol–gel reactions using as templates ionic and neutral surfactants. Wei et al. reported the use of low cost nonsurfactant organic compounds as pore forming agents, such as hydroxy acids and urea [3,4].

Mesoporous titania was first prepared using a phosphate surfactant through a modified sol–gel process [5]. However, products were not pure titanium dioxide because a significant amount of phosphorous still remained in these materials.

Antonelli et al. [6] have synthesized non phosphated mesoporous titania using dodecylamine as the directing agent and titanium isopropoxide as precursor. However, the porous structure has not been retained after the treatment in air at 300 °C.

The catalysts based on heteropolyacids have many advantages over liquid acid catalysts. They are noncorrosive and environmentally benign, presenting fewer disposal problems. Their repeated use is possible, and their separation from liquid products is easier than the homogeneous catalysts.

Acidic or neutral substances such as active carbon, SiO_2, ZrO_2 and TiO_2 are suitable as heteropolyacids supports [7,8]. Nevertheless, mesoporous titania has been scarcely used for this purpose.

The effect of thermal treatment on the structure and texture of mesoporous titania prepared using urea as low cost

* Fax: +54 221 4211353.
E-mail address: lrpizzio@dalton.quimica.unlp.edu.ar.

0167-577X/$ - see front matter © 2004 Elsevier B.V. All rights reserved.
doi:10.1016/j.matlet.2004.11.045

pore forming agent, via HCl catalyzed sol–gel reactions, is presented here. The acidic properties were measured by the thermal programmed desorption of chemisorbed pyridine.

2. Experimental

Titaniumisopropoxide (Aldrich, 26.7 g) was mixed with absolute ethanol (Merck, 186.6 g) and stirred for 10 min to obtain a homogeneous solution under N_2 at room temperature, then 0.33 cm^3 of 0.28 M HCl aqueous solution was dropped slowly into the above mixture to catalyze the sol–gel reaction for 3 h. After that, an appropriate amount of urea–alcohol–water (1:5:1 weight ratio) solution was added to the hydrolyzed solution under vigorous stirring to act as template. The amount of added solution was fixed in order to obtain a template concentration of 10 and 30 wt.% in the final material (Ti_L and Ti_H, respectively). The gel was kept in a beaker at room temperature till dryness. The solid was grounded into powder and extracted by distilled water for three periods of 24 h, in a system with continuous stirring to remove urea (Ti_{Lw} and Ti_{Hw}, respectively). Finally, it was calcined at 100, 200, 300 and 400 C during 24 h.

The samples were named according to the template concentration and calcination temperature (Ti_{L100}, Ti_{H100}, Ti_{L200}, Ti_{H200}, etc.).

The TG-DTA measurements of the solid were carried out using a Shimadzu DT 50 thermal analyzer. The thermogravimetric and differential thermal analysis were performed under argon or nitrogen, respectively, using 25–50 mg samples and a heating rate of 10 C/min. The studied temperature range was 20–700 °C.

The X-ray diffraction (XRD) patterns were recorded with a Philips PW-1732 equipment in the 5–60° 2θ range, using Cu Kα radiation and scanning speed of 1° per minute.

Fourier transform infrared (FT-IR) spectra of the solids were obtained in the 4000–1500 cm^{-1} wavenumber range using a Bruker IFS 66 FT-IR spectrometer.

The DRIFTS spectra were obtained using the same equipment. The samples were placed inside the chamber (Spectra Tech 0030-103) without dilution, with a N_2 stream of 50 cm^3 min^{-1}. For each spectrum, two hundred scans were obtained with 4 cm^{-1} resolution.

Specific surface area of the solids were determined from N_2 adsorption–desorption isotherms at liquid–nitrogen temperature. They were obtained using a Micromeritics Accusorb 2100E equipment. The samples were previously degassed at 100 °C for 2 h.

Pyridine adsorption tests were carried out at room temperature keeping in contact the samples with a pyridine saturated N_2 atmosphere. The excess and/or the physisorbed pyridine was evacuated at 100 °C. Before the adsorption experiments, the samples were kept in the same chamber at 100 °C under a N_2 stream of 100 cm^3 min^{-1} during 2 h, in order to eliminate the physically adsorbed water.

The total acidity of the samples was determined by thermal programmed desorption (TPD) of pyridine using the differential scanning calorimetry unit of a Shimadzu DT 50 thermal analyzer.

3. Results and discussion

The specific surface area (S_{BET}) of the solids determined from N_2 adsorption–desorption isotherms, together with the average pore diameter (D_P) obtained from the BJH pore size distribution, are shown in Table 1. As we can see, all the samples are mesoporous with a D_P greater than 3.2 nm. The S_{BET} decreased when increasing the calcination temperature (Table 1). Calcination at 300 and 400 °C produces little pore narrowing. Some of the narrowest pores seem to collapse upon the evolution of water forming two groups of pore size in the mesopore range.

On the other hand, Ti_H solids present higher S_{BET} than those of Ti_L solids calcined at the same temperature. From these results, it can be seen that S_{BET} increases with the increase of the urea content. However, the pore size distribution is practically the same. The most likely reasons for the effect of the urea concentration on the specific surface area and pore diameter are the number and the size of the template aggregates present during the sol–gel process. When the urea concentration increases, the number of aggregates increases, but their size does not change, as result a larger S_{BET} is obtained. Another reason could be the fact that the increment in the urea concentration changes the hydrolysis rate of titanium isopropoxide and the following polymerization step, as it was reported by Lopez et al. [9] when NH_4OH is used in the hydrolysis of titanium ethoxide.

The FT-IR spectra of Ti_{Hw} and Ti_{Lw} did not present any of the characteristic band of the urea, showing that the template was completely removed by water extraction.

The FT-IR spectra of Ti_{L100}, Ti_{L200}, Ti_{L300} and Ti_{L400} (Fig. 1) presented bands at 1618 and 3427 cm^{-1} assigned to the OH bending and stretching of water [10], which have been incorporated in the structure of the solid [11]. FT-IR spectra of Ti_{H100}, Ti_{H200}, Ti_{H300} and Ti_{H400} showed similar features to those observed for the Ti_L samples. For both series of samples (Ti_L and Ti_H), the intensities of the bands

Table 1
Textural and acidic properties of mesoporous titania

Sample	S_{BET} (m^2/g)	D_P (nm)	N_w (molecules/g)	PyAA (mmol/g)	TPD_{max} (°C)
Ti_{L100}	287	3.9	1.52×10^{21}	0.71	427
Ti_{L200}	221	4.0	1.11×10^{21}	0.66	414
Ti_{L300}	159	3.2–5.8	0.51×10^{21}	0.43	392
Ti_{L400}	124	3.9–5.9	0.38×10^{21}	0.34	390
Ti_{H100}	334	3.8	1.40×10^{21}	0.74	423
Ti_{H200}	290	3.9	1.02×10^{21}	0.69	411
Ti_{H300}	187	3.8–6.2	0.52×10^{21}	0.49	388
Ti_{H400}	157	3.6–6.5	0.39×10^{21}	0.36	387

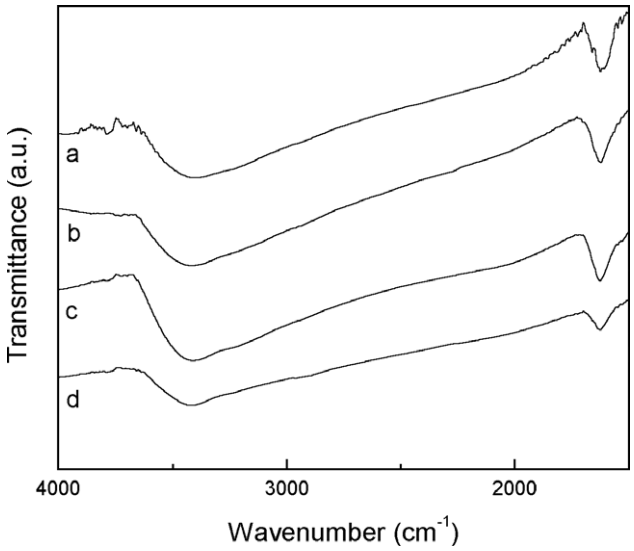

Fig. 1. FT-IR spectra of Ti_{L100} (a), Ti_{L200} (b), Ti_{L300} (c) and Ti_{L400} (d) samples.

decreased when the calcination temperature increased in parallel with the reduction of the S_{BET}.

The DTA diagrams of Ti_{L100} and Ti_{H100} showed an endothermic peak at 52 and 50 °C, respectively, associated with the loss of physically adsorbed water, and two poorly developed endothermic peaks at 310 and 370 °C (305 and 358 °C for Ti_{H100} sample) attributed to the partial dehydroxylation of the titania surface. They could be considered as an indication of the presence of two types of hydroxyls in the titania surface [12]. DTA diagrams of Ti_{L200} (Ti_{H200}) and Ti_{L300} (Ti_{H300}) samples presented similar features to those of Ti_{L100} and Ti_{H100}, respectively. However, for Ti_{L400} and Ti_{H400} samples, the endothermic peaks assigned to dehydroxylation were absent.

TGA patterns show that dehydration takes place in two main steps. The first step is due to the loss of physically adsorbed water (below 160 °C) and the second to the loss of structural water in the temperature range 160 to 400 °C. For the Ti_{L100} and Ti_{H100} samples, the number of water molecules released per gram (N_w) estimated from the weight loss ascribed to the second step was 1.52×10^{21} and 1.40×10^{21}, respectively. N_w decreased when the calcination temperature of the Ti_L and Ti_H increased (Table 1), as result of the dehydroxylation of the titania surface during the thermal treatment of the samples.

The XRD pattern of Ti_{L100} (Fig. 2) exhibits only the characteristic peaks of anatase phase at 2θ=25.3° (101), 37.9° (004), 47.8° (200) and 54.3°. The pattern does not present low angle diffraction peaks, characteristics of ordered mesoporous structures. The crystallinity of the samples increased when the temperature went up and the peak at 54.3° splitted into two peaks at 54.0° (105) and 54.9° (211) when the temperature was over 200 °C.

The XRD pattern of Ti_{H100} was quite similar to that of the Ti_{L100} sample and the same behavior with the increment of the temperature was observed.

The TPD patterns of adsorbed pyridine from titania samples present one broad desorption peak with maximum (TPD_{max}) in the temperature range 390–426 °C. The total amount of pyridine adsorbed estimated from the TGA curves (PyAA) decreases in parallel with the increase of the calcination temperature (Table 1).

The chemisorption of pyridine followed by IR studies is usually a useful probe for the presence and nature of surface Lewis acid and Brønsted acid sites on a catalyst surface [13]. According to Knozinger [14], the ring-stretching vibrational modes of pyridine that are most affected through such intermolecular interactions are originally at 1439 and 1583 cm^{-1} [15]. These two modes are observed, at 1535–1550 and about 1640 cm^{-1}, respectively, for pyridinium ion (PyH^+) and at 1440–1460 and 1600–1635 cm^{-1} for pyridine coordinatively bonded to Lewis acid sites (PyL). Information on the strength of Lewis and Brønsted acid sites can be obtained from pyridine thermodesorption experiments.

The DRIFTS spectrum of the Ti_{L100}Py sample (Fig. 3b) displayed bands at 1146, 1222, 1441, 1488, 1541 and 1589 cm^{-1} that were not present in the Ti_{L100} sample (Fig. 3a). The band at 1541 cm^{-1} could be assigned to PyH^+ as a result of the interaction between strong proton centers (OH groups and coordinated H_2O molecules) on the Ti_{L100} surface and pyridine molecules [16,17], but only when the absorption band at about 1640 cm^{-1} is also present [18]. In the Ti_{L100}Py sample, the bending band of water at 1635 cm^{-1} does not allow its detection. For this reason, it is not possible to conclude accurately that Brønsted acid sites are present on the sample.

On the other hand, Parfitt et al. [18] assigned the bands at 1222, 1441 and 1589 cm^{-1} to the presence of Lewis acid cites of Type I, which strongly adsorbed pyridine. At the same time, they ascribed the band at 1146 cm^{-1} to Lewis acid cites of Type II, to which pyridine was weakly

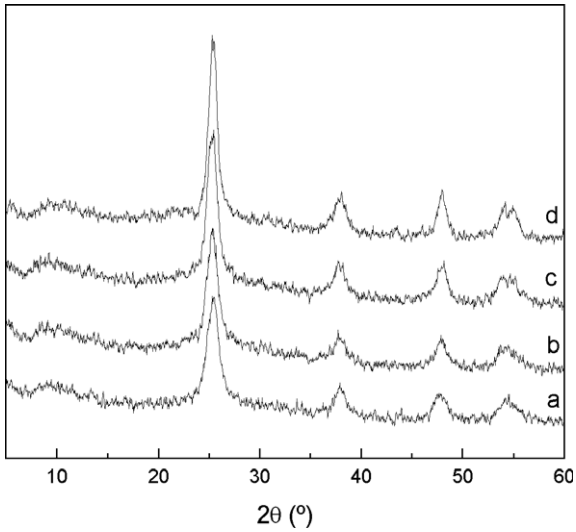

Fig. 2. XRD patterns of Ti_{L100} (a), Ti_{L200} (b), Ti_{L300} (c) and Ti_{L400} (d) samples.

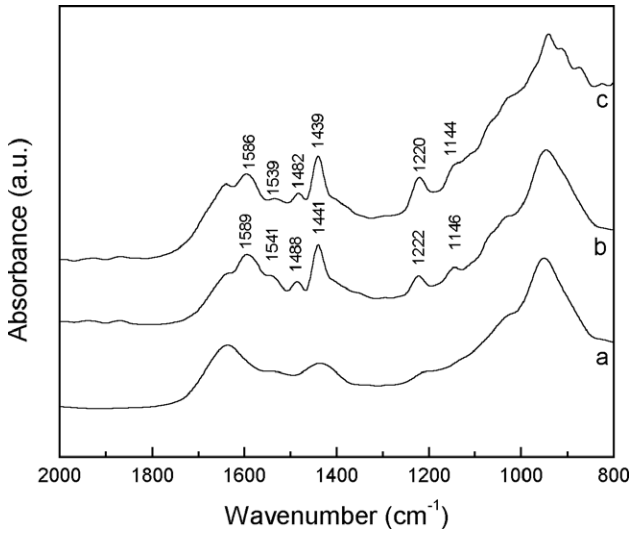

Fig. 3. DRIFTS spectra of Ti_{L100} (a), $Ti_{L100}Py$ (b) and (c) $Ti_{H100}Py$ samples.

coordinated. According to Bezrodna et al. [16], the band placed at 1488 cm^{-1} could be due to pyridine interactions with both Lewis and Brønsted active sites.

For hydrogen bonded pyridine, the ring-stretching vibrational modes are observed at 1440–11450 and about 1580–1600 cm^{-1}, respectively, only if the evacuation temperature was lower than 200 °C [19]. Recently, Zaki et al. showed that hydrogen bonded species were completely eliminated outgassing titania samples at temperatures ≥27 °C [17]. In this work, the samples were evacuated at 100 °C and according to the TPD studies, the desorption of pyridine becomes significant when the temperature is over 250 °C. So, it is possible to rule out the presence of hydrogen bonded pyridine in the samples.

The same set of bands was present in the DRIFTS spectrum of $Ti_{H100}Py$ sample (Fig. 3c), although some of them displayed its maximum at slightly lower wavenumber. The DRIFTS spectra of the $Ti_{L200}Py$ ($Ti_{H200}Py$), $Ti_{L300}Py$ ($Ti_{H300}Py$) and $Ti_{L400}Py$ ($Ti_{H400}Py$) samples were quite similar to that of $Ti_{L100}Py$ ($Ti_{H100}Py$). However, the intensity of the band at 1541 cm^{-1} decreased when the calcination temperature increased, in parallel with the decrease of the number of structural water molecules released per gram (N_w), as result of the partial dehydroxylation that takes place during the thermal treatment of the samples.

4. Conclusions

Mesoporous titania materials have been prepared using urea as pore forming agent, via HCl catalyzed sol–gel reactions. The specific surface area of titania samples depend on the urea concentration used during the synthesis and decrease with the increment in the calcination temperature.

The study of the samples by DRIFTS allows us to verify that the bands ascribed to pyridine adsorption on Lewis acid sites are present. The presence of Brønsted acid sites was not able to be determined with accuracy on the sample.

According with DSC-TGA measures, the acidity estimated from the total amount of pyridine adsorbed decreases with the increase of the calcination temperature as a result of the dehydroxylation of the titania surface.

Based on these results, the mesoporous titania samples synthesized present suitable properties to be used as carrier in the preparation of heteropolyacids supported catalysts, which are very attractive for many processes in replacement of conventional liquid catalysts.

Acknowledgments

The author is very grateful to Dr. J. Sambeth, Ing. E. Soto and L. Osiglio for their experimental contribution, and to UNLP for the financial support (X224, X312 and X316 projects).

References

[1] T. Yanagisawa, T. Shimizu, K. Kuroda, C. Kato, Bull. Chem. Soc. Jpn. 63 (1990) 988.
[2] C.T. Kresge, M.E. Leonowicz, W.J. Roth, J.C. Vartuli, J.S. Beck, Nature 359 (1992) 710.
[3] Y. Wei, D. Jin, T. Ding, W.H. Shih, X.H. Liu, S.Z.D. Cheng, Q. Fu, Adv. Mater. 3 (1998) 313.
[4] J.Y. Zheng, J.B. Pang, K.Y. Qiu, Y. Wei, Microporous Mesoporous Mater. 49 (2001) 189.
[5] D.M. Antonelli, J.Y. Ying, Angew. Chem., Int. Ed. Engl. 34 (1995) 2014.
[6] D.M. Antonelli, Microporous Mesoporous Mater. 30 (1999) 315.
[7] L.R. Pizzio, C.V. Cáceres, M.N. Blanco, Appl. Catal. 167 (1998) 283.
[8] L. Pizzio, P. Vázquez, C. Cáceres, M. Blanco, Catal. Lett. 77 (2001) 233.
[9] T. López, E. Sánchez, P. Bosch, Y. Meas, R. Gómez, Mater. Chem. Phys. 32 (1992) 141.
[10] J. Rubio, J.L. Otero, M. Villegas, P. Duran, J. Mater. Sci. 32 (1997) 643.
[11] J.A.R. Van Veen, F.T.G. Veltmaat, G. Jonkers, J. Chem. Soc., Chem. Commun. (1985) 1656.
[12] S.A. Selim, Ch.A. Philip, S. Hanafi, H.P. Boehm, J. Mater. Sci. 25 (1990) 4678.
[13] E.P. Parry, J. Catal. 2 (1963) 371.
[14] H. Knozinger, in: D.D. Eley, H. Pines, P.B. Weisz (Eds.), Advances in Catalysis, vol. 25, Academic Press, New York, 1976, p. 184.
[15] F.R. Dollish, W.G. Fately, F.F. Bentley, Characteristic Raman frequencies of organic compounds, Wiley, New York, 1974.
[16] T. Bezrodna, G. Puchkovska, V. Shimanovska, I. Chashechnikova, T. Khalyavka, J. Baran, Appl. Surf. Sci. 214 (2003) 222.
[17] M.I. Zaki, M.A. Hasan, F.A. Al-Sagheer, L. Pasupulety, Colloids Surf., A 190 (2004) 261.
[18] G. Parfitt, J. Ramsbotham, C. Rochester, Trans. Faraday Soc. 581 (1971) 1500.
[19] M.C. Kung, H.H. Kung, Catal. Rev., Sci. Eng. 27 (1985) 425.